AN ABSTRACT OF THE THESIS OF

Frank John Weber for the degree of Master of Science in Materials Science presented on October 31, 1995. Title: Changes in Structure and Stress in Mo/a-Si Thin Films upon Annealing.

Redacted for Privacy

Abstract approved: _____

Michael E. Kassner

The structural and stress changes in molybdenum/amorphous silicon (Mo/a-Si) EUV reflecting multilayers during annealing at 316°C were studied. The amorphous interlayers, with an Mo:Si stoichiometry of 1:2, grew during annealing. The residual stresses in each component of the multilayer also changed significantly. Through high resolution electron microscopy, selected area electron diffraction, and x-ray diffraction of the crystalline Mo, the biaxial tensile stresses were shown to increase from approximately two to about ten GPa in the lateral direction, parallel to the interface plane. The compressive strains developed in the vertical direction, perpendicular the interface plane, are consistent with a Poisson contraction calculated from bulk elastic properties. Laser deflectometry measurements of thicker (non-EUV, 0.1μm) amorphous silicon showed compressive stress relaxation in the amorphous silicon with annealing, which may also take place in the thin (EUV) silicon. The residual stress in a 40 bilayer EUV film changes from about -0.5 GPa to about +1.5 GPa.

Changes in Structure and Stress in Mo/a-Si Thin Films upon Annealing

by

Frank John Weber

A THESIS

submitted to

Oregon State University

in partial fulfillment of
the requirements for the
degree of

Master of Science

Completed October 31, 1995
Commencement June 1996

Master of Science thesis of Frank John Weber presented on October 31, 1995

APPROVED:

Redacted for Privacy

Major Professor, representing Materials Science

Redacted for Privacy

Chair of the Material Science Program

Redacted for Privacy

Dean of Graduate School

I understand that my thesis will become part of the permanent collection of Oregon State University libraries. My signature below authorizes release of my thesis to any reader upon request.

Redacted for Privacy

Frank John Weber, Author

DEDICATION

I dedicate this thesis to my parents, Johann Weber and Elisabeth Weber, and to my sister, Christine Weber-Fox, for their love and support.

ACKNOWLEDGMENTS

I thank M.E. Kassner and D.G. Stearns for their guidance and assistance. I also thank J. Koike, R.S. Rosen and S.P. Vernon for their assistance. Thanks to thank M. Villiardos for measurement of the interlayer thickness and Y. Cheng of Arizona State University for x-ray diffractometer experiments. I also wish to thank Professor W.D. Nix and V.T. Gillard for help with the Stanford laser deflectometer. Financial support for this work came from Lawrence Livermore National Laboratory to Oregon State University.

TABLE OF CONTENTS

LIST OF FIGURES

LIST OF TABLES

Changes in Structure and Stress in Mo/a-Si Thin Films upon Annealing

INTRODUCTION

Extreme ultraviolet (EUV) reflecting mirrors can be made from a series of thin film bilayers. One layer of the bilayer has a high atomic scattering factor while the other a low scattering factor. Molybdenum/amorphous silicon (Mo/a-Si) multilayers are an example of high reflectivity EUV mirrors. The reflectivity of these multilayered films is greatly affected by the interfaces between the layers. Ideal interfaces are smooth with an abrupt composition change from one layer to the other. Roughness of the interface and/or the formation of diffuse interlayers degrade the reflectivity. Also, changes in the bilayer thickness due to interdiffusion and growth of the interlayer modifies the x-ray wavelength at which peak reflectivity is achieved [1].

An Mo/a-Si 40-bilayer film with 3 nm Mo, 4 nm a-Si, and ideal interfaces would have a theoretical peak reflectivity of about 70 percent for EUV radiation with a 13 nm wavelength at normal incidence. The actual peak reflectivity achieved is about 66 percent, reduced at least partly due to the formation of amorphous interlayers during deposition, which have a Mo:Si stoichiometry of about 1:2. Annealing the multilayers at temperatures up to 300-400°C causes growth of the interlayers and their eventual crystallization, leading to further degradation of the reflectivity [2,3].

Thin films are often in a state of high residual stress. These films often have a non-equilibrium structure and are deposited at temperatures different from application temperatures, giving rise to thermal stress. An EUV reflective optic coated with such a film could be significantly distorted and, with a sufficiently thick film, fracture and flaking of the film may occur. Microstructural changes during annealing are expected to alter the stress state in multilayers. Some residual stress measurements on Mo/a-Si multilayers with relatively thick individual layers have been performed by Kola et al. [4]. The stress in the

films was determined using laser deflectometry which measures the change in curvature of substrates that are relatively thick. This method is more precise for relatively thick deposited layers (e.g. > 100 nm) than for thin layers (<5 nm). Since residual stresses may depend on the thickness of the crystalline layers, other techniques may be superior for EUV multilayers. The defect structure and stress state may change in crystalline materials as the thickness increases beyond roughly 5 nm (larger than the layers in the multilayers of this study) due to the mobility of misfit dislocations in thicker layers [5]. Thus thick crystalline layers may more easily plastically deform by dislocation motion resulting in residual stress states lower than those in multilayers with the layer thicknesses of this investigation. Furthermore, Nguyen et al. [6,7] have shown that the structure of a film may change with thickness, thus changing the average residual stresses. Thus, the stress behavior in crystalline phases with annealing and cooling shown by Kola et al. may not be applicable to optical-scale multilayers.

The elastic strains can be determined in relatively thin layers (< 5 nm) using high resolution electron microscopy (HREM), selected area electron diffraction (SAED), and x-ray diffraction (XRD) for crystalline materials. XRD has been used by others on thin-layer multilayers [8] whereas the other techniques are less commonly used. Film stresses may be calculated form the obtained strains assuming that the elastic properties of the film are accurately known. Of course, diffraction methods cannot be used for residual stress measurements in amorphous materials. However, laser deflectometry can be used, assuming no thickness effects on amorphous film structure, and residual stresses then calculated. As will be discussed later, the thickness effect on film stress may be suppressed when using a layering technique described by Nguyen [6]. Furthermore, average stress in an EUV multilayer, which consists of 40 bilayers, can be determined by laser deflectometry. Knowledge of the average stresses in the multilayer, Mo, and the thin amorphous silicon layers can thus be used to calculate the residual stresses in the $MoSi_2$ interlayer.

This study investigated the thermal stability of reflective Mo/a-Si multilayers by examining changes in the microstructure and stress state during annealing at 316°C, complementing earlier preliminary structural studies by others at other temperatures [1,2]. Attempts were made to relate residual stress and microstructural alterations with elevated temperature exposure.

EXPERIMENTAL PROCEDURE

The multilayers of this study that are used for EUV mirrors consist of 40 bilayers of Mo/a-Si consisting of nominally 3 nm Mo and 4 nm a-Si deposited on (100) oriented single crystal silicon wafers. The native oxide on the wafers was not removed. The deposition was performed using a d.c. magnetron sputter deposition system schematically shown in Figure 1. The substrate to be coated is mounted face down on a small platter driven by a d.c. servomotor. This motor in turn is mounted on a platter with the substrate poking through a hole in the platter. Spinning the substrate at about 4 rev/sec as it passes over the sputtering targets insures uniformity. The platter is mounted to a column which is mounted to a Ferrofluidic^{TM} rotary feedthrough in the chamber lid. A computer controlled stepper motor drives the platter through an overall reduction of 100:1. Given a certain deposition rate from the magnetrons, the layer thicknesses are controlled by the speed of passage over the targets. The magnetron sources are mounted in the bottom of the chamber face up and are water cooled. An array of magnets underlying the sputtering targets, and giving a field strength of about 300 gauss at the target surface, helps to confine the plasma. Sputtering action is kept from the sides of the magnetron with a ground shield surrounding the periphery of the target. Material sputtered off the target is mostly confined to the volume above the target by means of chimneys that reach close to the platter rotating overhead.

The magnetron guns were operated in constant power mode and are quite stable. Argon boiled off from a large dewar was used as the sputtering gas. Flow was maintained at 14 SCCM and pressure was maintained at 1.75 mtorr. The silicon gun (magnetron) was operated at 280 W and the Mo gun was operated at 110 W. The silicon target was dopedwith 10 ppm of boron for sufficient conductivity. The deposition rate was calibrated by coating several trial substrates at various speeds and then determining the bilayer thickness using small angle x-ray diffraction. This diffraction was done using a Rigaku DMAX diffractometer at LLNL using Cu K-α radiation ($\lambda = 0.1542$ nm).

Figure 1 Schematic of Sputter Deposition system

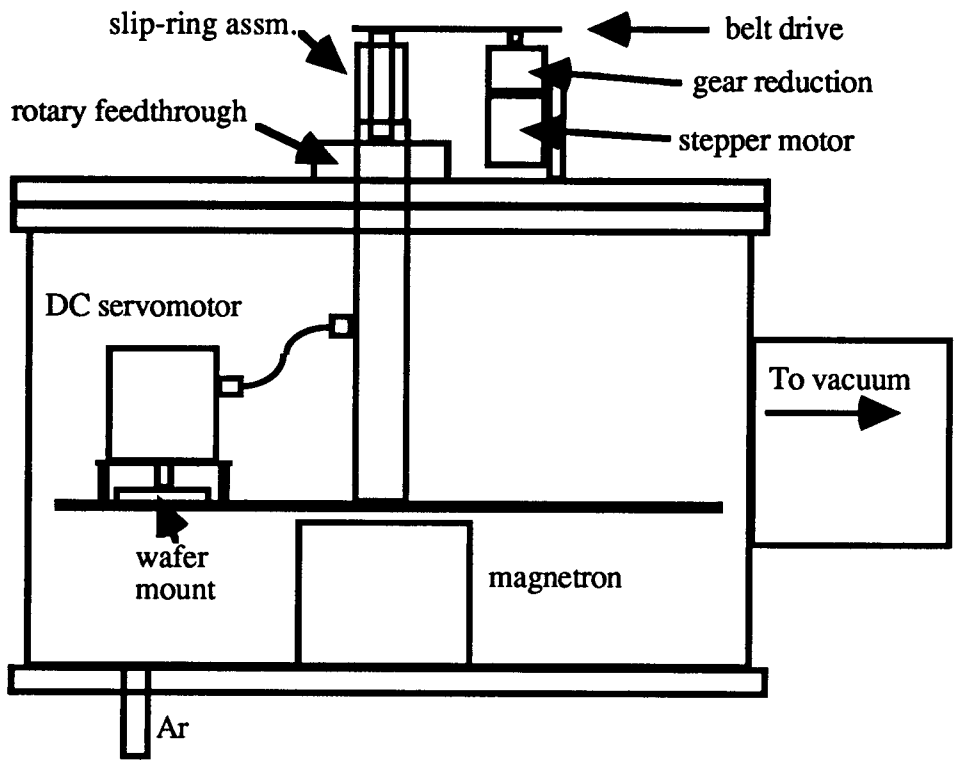

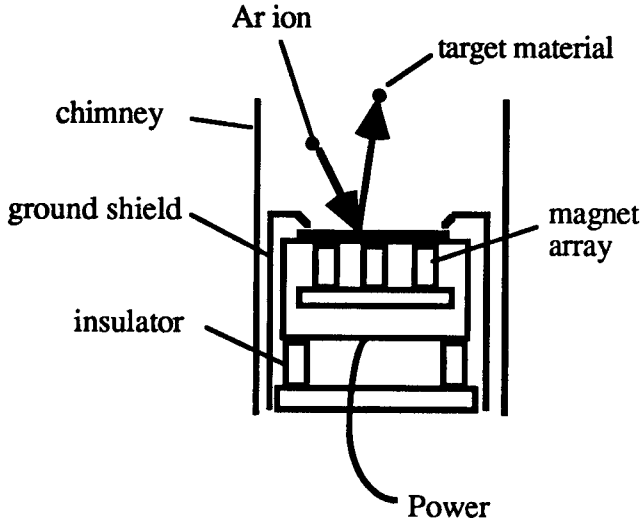

Three, relatively thick mono-, bi-, and trilayered films were also deposited for additional laser diffractometer curvature measurements. The three layer configurations were: a-Si on substrate, Mo on a-Si on substrate, and a-Si on Mo on a-Si on substrate. Layers of about 0.1 μm (Si was 0.11μm and Mo was 0.105μm) were deposited on 350 μm thick, 100 mm diameter (whole), silicon single crystal <100> oriented wafers. The deposition conditions for the thick and thin layers were identical, except that the increased thickness was achieved by multiple passes over a given sputtering target. Thicknesses for these were not measured but were assumed to be equal to the thickness resulting from multiplying the number of passes by the thickness that would be obtained in each thin layer assuming no interlayer formation.

To coat a wafer, the deposition chamber would be loaded and then evacuated overnight to a pressure near 3×10^{-7} torr. Residual gas analysis showed this to be mostly water vapor. This means that a monolayer of water may be adsorbed on the surface during the ~10 second pass intervals between sputtering targets. Therefore, there was concern that the thick-film data in this work is not necessarily reflective of pure material of identical thickness. However, the investigation of Nguyen [6] appears to suggest that such a "layering" technique, for a pure material, such as Mo, is a means to maintain the structure of thin (nm-scale) films in thicker (μm-scale) films. Nguyen presents evidence that over the thickness range of about 5 nm to 1μm , a-Si residual stresses may change by about a factor of two for unlayered, single element, films. This is not a dramatic change and our "layering" or multipass technique may minimize this effect.

The EUV multilayers used for the thermal stability study and examined by HREM, SAED and XRD were cleaved into relatively small (approximately 12 mm x 24 mm) sections and annealed for various periods at 316°C, up to 100 hours. They were sealed in Pyrex tubes and evacuated to less that 10^{-5} torr to minimize oxidation during annealing. The whole wafers used for curvature measurements at Stanford University were annealed at 316°C for 1/2 hour and 10 hours. Since these wafers were 100 mm in diameter, the

encapsulating tubes were relatively large (100 mm dia., 300 mm long). Thus the time to reach 316°C was longer, approximately 15 minutes as compared to about 5 minutes for the smaller samples, as measured with a thermocouple. This increases uncertainty of the 1/2 hour annealing time for the whole wafers relative to that of the cleaved specimens. The cleaved (15 mm x 5 mm) wafers used for curvature measurements at Tohoku University in Sendai, Japan, were annealed at 316°C for 0.33, 0.67, 1,5, and 25 hours, at 10^{-7} torr.

Specimens examined using HREM and SAED were mechanically polished, ion milled to perforation using a Gatan model 600 dual ion mill, and then examined with a JEM 4000 EX transmission electron microscope at Arizona State University. Mo-Si interlayer thickness changes due to growth during annealing were determined using high resolution lattice fringe images that were recorded on photographic plates, digitized and converted to 256 gray-scale images. The layers and interlayers could then be identified by their range of gray-scale values. A single color was assigned to each range to aid in thickness measurements, which were performed at several location in each image.

The {110} and {100} plane spacings were measured to determine lateral (parallel to the layers) and {110} vertical (perpendicular to the layers) strains in the Mo. The polycrystals of Mo were oriented (textured) such that <110> directions were parallel to the multilayer normal. The lateral spacing was measured using conventional SAED. An entire multilayer was included in the aperture for the SAED pattern. This resulted in strong superlattice spots aligned in the vertical direction, which overlapped the transmission spot. Each crystalline spot had an intensity streaked in the vertical direction due to the effect of Mo layer thickness on the diffraction-intensity distribution. Therefore, the lateral diffraction pattern spacing, but not the vertical spacing, could be measured using SAED. The {110} and {100} lattice spacings were obtained from the diffraction patterns using Bragg's law. The specimens were oriented to maximize diffraction intensity so as to minimize deviation from the Bragg condition when recording SAED patterns. This generally limits the uncertainty of the lattice parameter measurements to approximately

±0.3%. Several diffraction patterns were taken from the Si substrates to calibrate the camera constant. Error bars in the figures were defined by the average range between maximum and minimum lattice parameters in each specimen.

Vertical spacings were obtained from diffraction patterns that were derived by fast Fourier transformation (FFT) of the digitized lattice fringe images. The pattern derived by FFT avoided the superlattice spots by using only a single Mo layer in the analysis. The lattice fringe images on the photographic plates were digitized using a CCD camera connected to a computer. Well-defined fringes were observed predominantly in the lateral direction due to the texturing of the Mo (<110> in the vertical direction). A 5 nm by 5 nm area over a layer, showing well defined {110} lattice fringes parallel to the interface, was chosen for FFT. The FFT of the periodic {110} lattice fringes resulted in sharp 110 diffraction spots in the vertical direction. An iterative procedure was used to determine the maximum intensity of each spot. Lattice fringes and corresponding FFT patterns of the Si substrate in the same image were used to calibrate the camera constant. Since the lateral extent of an Mo grain in the film was around 5 nm, this technique could yield the strains in a single grain.

In order to supplement the FFT technique, which utilizes perforated thin foils, vertical elastic strains were also measured with an x-ray diffractometer with a Cu K-alpha source ($\lambda = 0.154$ nm). The advantage of this technique is that the strains are measured for a thin film in its intended configuration, as opposed to that in a highly prepared specimen. The x-ray measurements were performed in the θ-2θ geometry on a Rigaku DMAX-IIB diffractometer (instrumental resolution of 0.1°). The specimens were scanned from 2θ = 36° to 46° to include the Mo {110} peak. Due to a slight asymmetric peak shape, the peak position was determined at the strongest intensity. The peak assymmetry was negligible for annealing times less than five hours. If peak position is determined by the full-width, half-maximum method, the strains determined at longer annealing times increase by a factor

of 1.2-1.3. These measurements were performed at Arizona State University to an accuracy of $\pm$0.6%.

The wafer curvature measurements were performed using a laser deflectometer at Stanford University, schematically shown in Figure 2, and at Tohoku University in Sendai, Japan. The beam is scanned across the substrate and finally strikes a lateral effect photodiode. For a perfectly flat substrate the beam does not change position on the diode. For a curved substrate, the change in position across the diode is proportional to the change in angle as it moves across the substrate surface. A plot of diode spot position versus substrate spot position for a uniformly curved substrate would then yield a straight line. The analysis of curvature and the associated stresses in layers deposited on substrates is described by Townsend et al. [10]. The stress in a film, for a film thickness much less than the substrate thickness, is given by:

$$\sigma = \frac{M_{<100>} t_s^2}{6 t_f} \Delta K \qquad (1)$$

where σ is the biaxial stress in the plane of the film, $M_{<100>} = C_{11} + C_{12} - 2C_{12}^2 / C_{11}$ is the biaxial modulus for a <100> oriented cubic substrate, t_s is the substrate thickness, t_f is the film thickness and ΔK is the change in substrate cuvature. The stress in each thick layer was determined by measuring the change in curvature after the deposition of each layer.

Figure 2 Schematic of laser deflectometry system

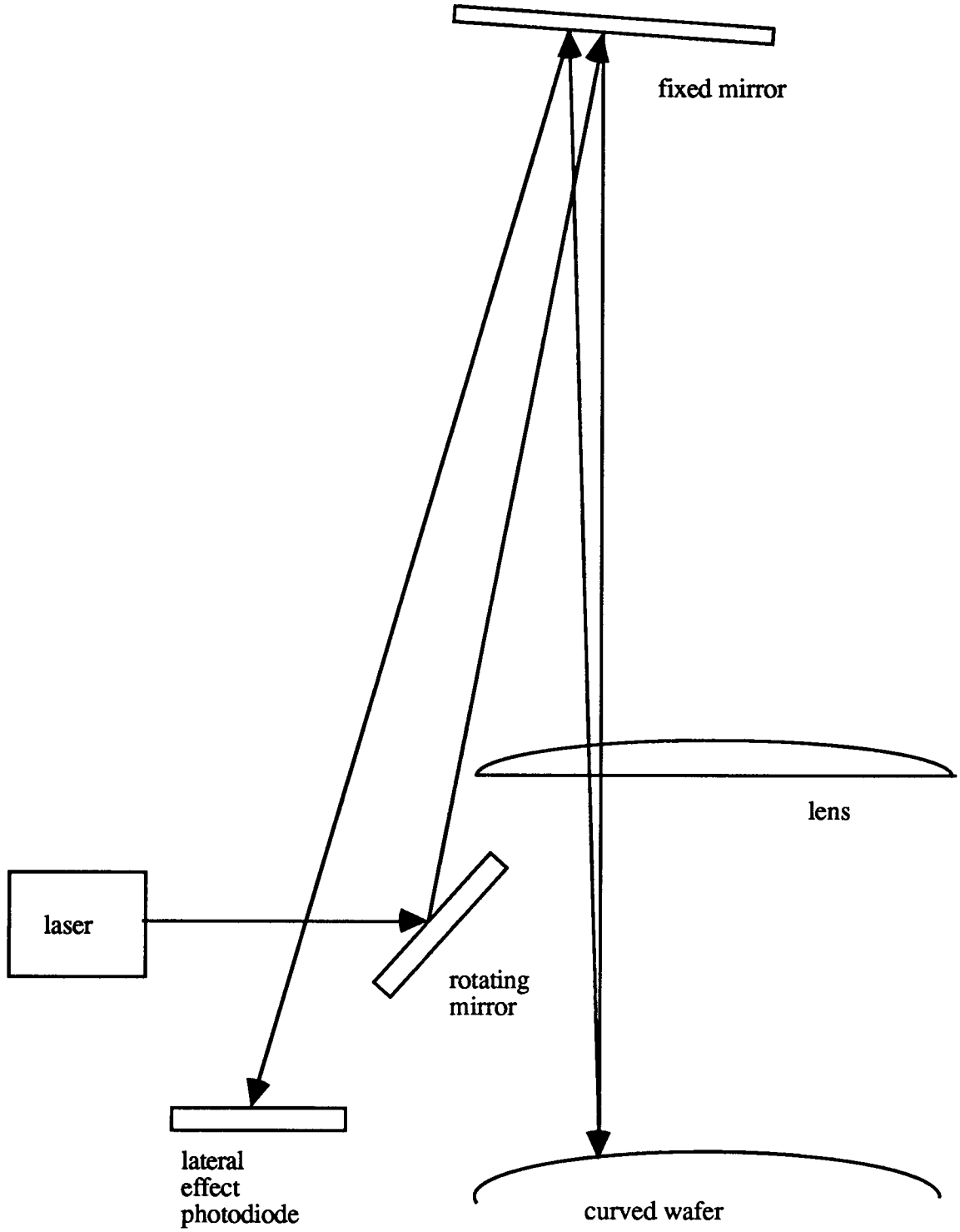

RESULTS AND DISCUSSION

An HREM image of an as-deposited multilayer is illustrated in Figure 3(a). The dark layers are Mo and the faint layers are a-Si. An intermediate shade of the amorphous a-Mo-Si interlayers are between these layers. The average Mo layer thickness was 2.33 nm and the average a-Si layer thickness was 3.06-nm for unannealed multilayers. The amorphous Mo-Si interlayers were 0.5 nm thick where Si was deposited on Mo and 1.0 nm thick where Mo was deposited on Si. An explanation for the difference in thicknesses of the interlayers is unclear, although others have also observed this disparity [11,12]. Lattice fringes approximately parallel to the interfaces, corresponding to {110} type planes, are observed in the Mo layers. This indicates texturing with <110> directions perpendicular to the deposition plane, as mentioned previously. Lateral grain dimensions of the Mo polycrystals vary from 5 to 30 nm.

Figures 3(b-d) shows a multilayer after 1 to 100 hour anneals at 316°C. The a-Mo-Si interlayer thicknesses have increased with annealing time. Earlier work showed that the decreases in thickness of the Mo and Si layers was consistent with the increase in the amorphous interlayer thickness providing a Mo:Si stoichiometry of 1:2 (and that the densities of crystalline and amorphous Mo-Si are nearly equal) [3]. Thus, the stoichiometry of the amorphous Mo-Si is probably 1:2.

The growth of the thick (Mo on a-Si) interlayer as a function of annealing time is shown in Figure 4. The thick interlayer rapidly grows from 1 nm to 1.4 nm in less than one hour, then gradually grows to 1.8 nm by 50 hours. The thin interlayer behaves similarly, with relatively rapid growth from 0.5 to 0.8 nm in one hour, followed by gradual growth to 1.0 nm over 50 hours. The secondary, gradual growth stage, has been shown to be controlled by the diffusion of Si through the interlayer to the Mo layer [1,2,13-15]. Crystalline hexagonal (h-) $MoSi_2$ forms during annealing [3]. Figure 5 shows the volume fraction of the crystallized $MoSi_2$ as a function of annealing time. These are based on area

Figure 3 HREM microrgraphs of multilayers at 0, 1, 10 and 100 hours of annealing.

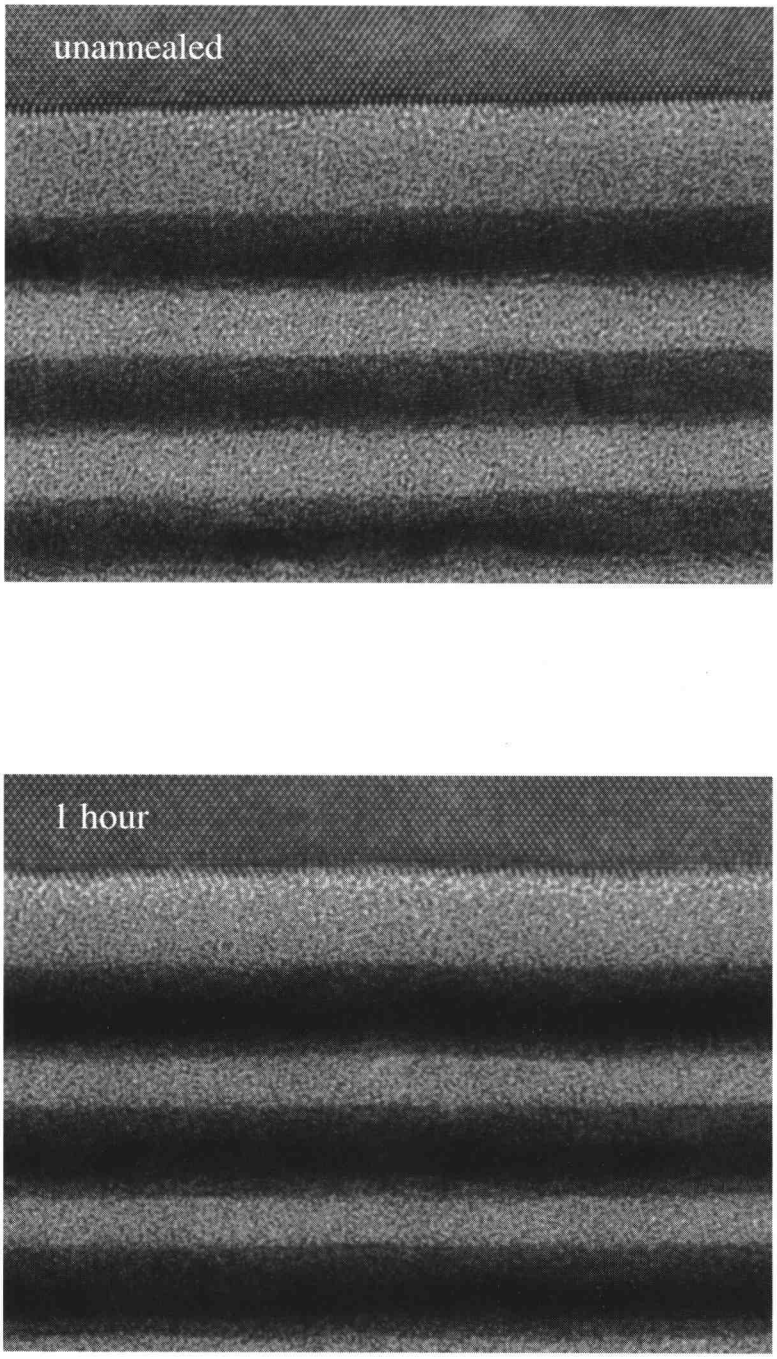

Figure 3 continued.

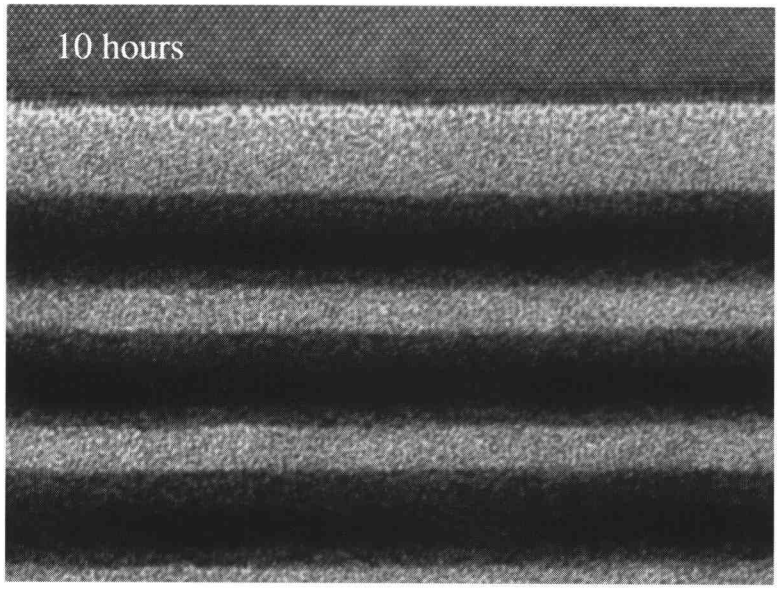

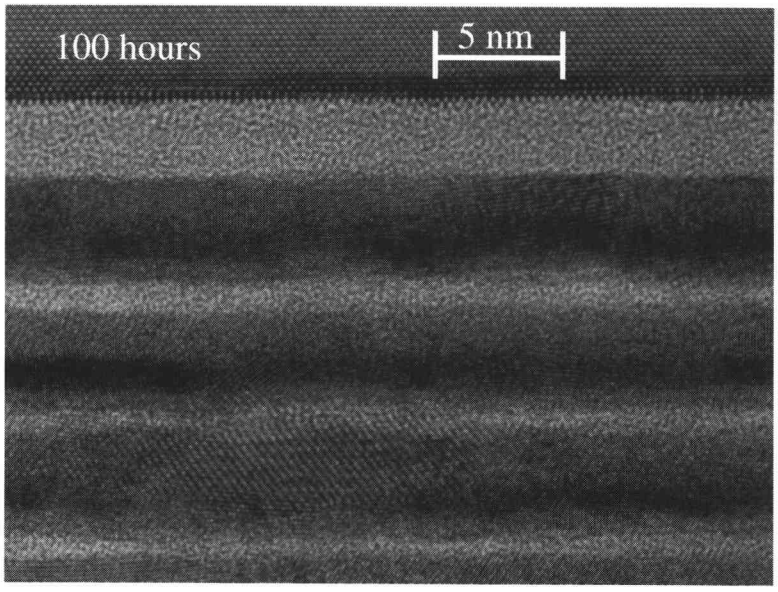

Figure 4 Interlayer growth as a function of annealing time.

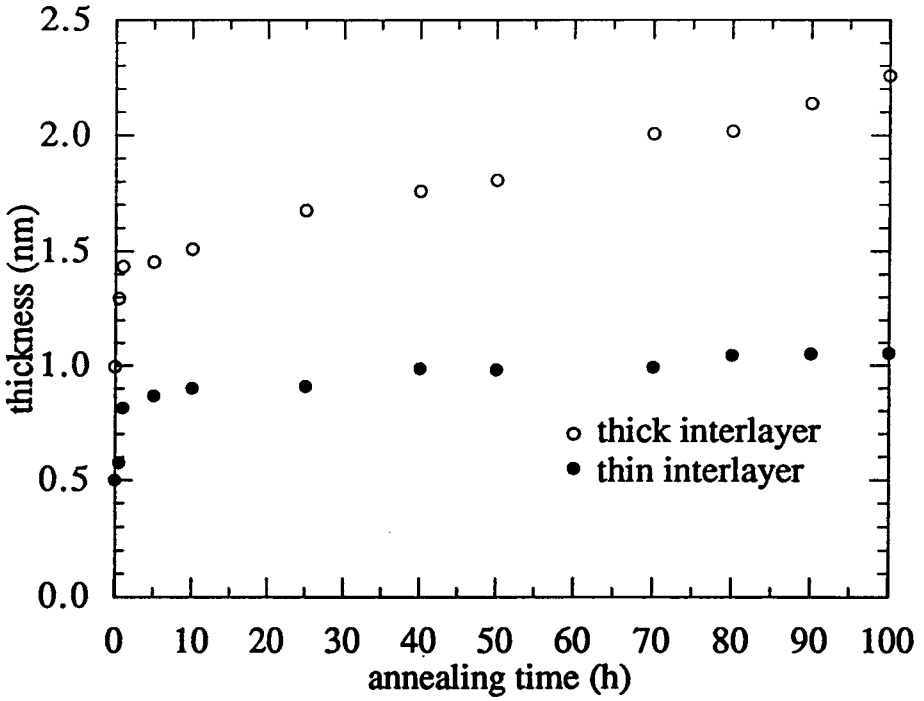

Figure 5 Percent crystallinity of interlayer as a function of annealing time.

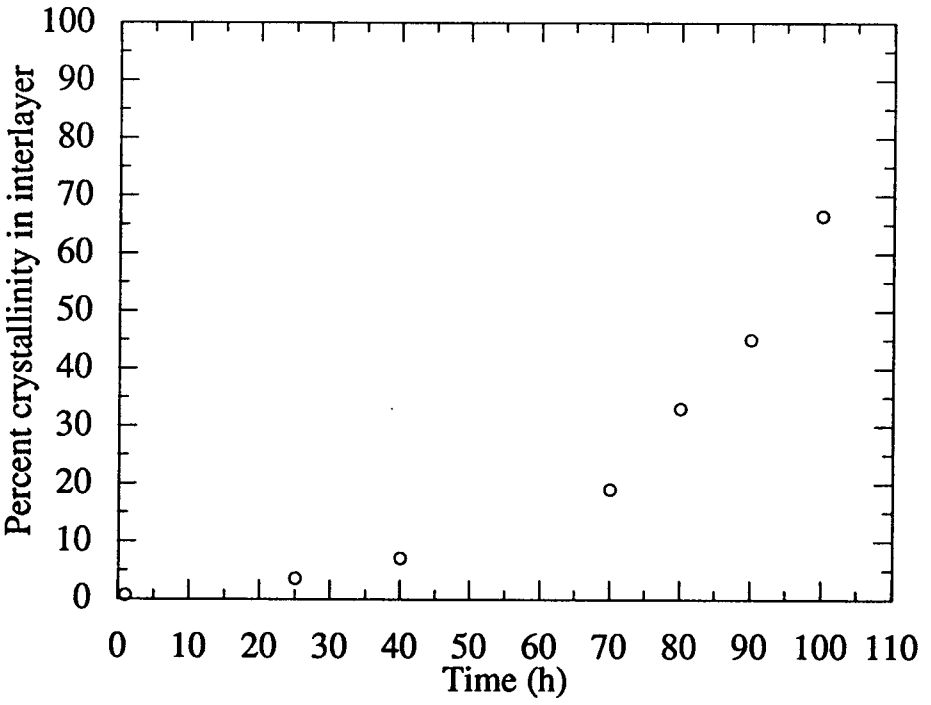

fractions crystallized as determined from the HREM images. Since some crystallites were not oriented to exhibit lattice fringe contrast, the values in the figure may be lower than the actual fraction of the crystallites. After about 100 hours, the interlayers appear to have nearly completely transformed to h-$MoSi_2$, although only 80% crystallization was confirmed. The crystallized volume after 50 hours of annealing is only 10%. As will be discussed subsequently, these results suggest that the effects of crystallization are not of primary importance in residual stress development.

Figures 6(a) and (b) show the lateral Mo $(01\bar{1})$ and (100) lattice spacings, determined by SAED as a function of annealing time. There is less (100) data due to uncertainty of (100) reflection images. Figure 6(c) shows the vertical (011) spacing determined using HREM/FFT and XRD, also as a function of annealing time. The HREM/FFT and XRD are in reasonable agreement, although the lattice parameters from the latter technique may be somewhat larger (predicting smaller strains). The dashed line is the spacing for bulk, unstressed, Mo. There is a rapid increase in lateral tensile strain during the first 5 hours followed by a more gradual increase. The vertical lattice spacing behaves similarly but with a compressive rather than a tensile sense. The associated stresses will be discussed later. Figure 7(a) and (b) shows the lateral and vertical strains versus annealing times based on the data of figure 6.

The stresses in the thick layers, as measured by deflectometry are listed in Table 1. Significant compressive stresses in the amorphous silicon deposited on the substrate decrease with annealing, consistent with the findings by others [4,16]. Interestingly the layered 0.1 μm a-Si has a residual stress comparable [6] to that of single thin films of comparable thickness to the a-Si layers in the optical (EUV) multilayer. The stress in the Mo layer deposited on a-Si is tensile as with the optical multilayer case. However, relaxation occurs in the thick layered film in contrast to the thin Mo layers of the optical multilayer. The stress relaxation in 0.1 μm a-Si layer deposited on Mo is comparable to that for a-Si on the substrate.

Figure 6 Mo lattice spacings as a function of annealing time.

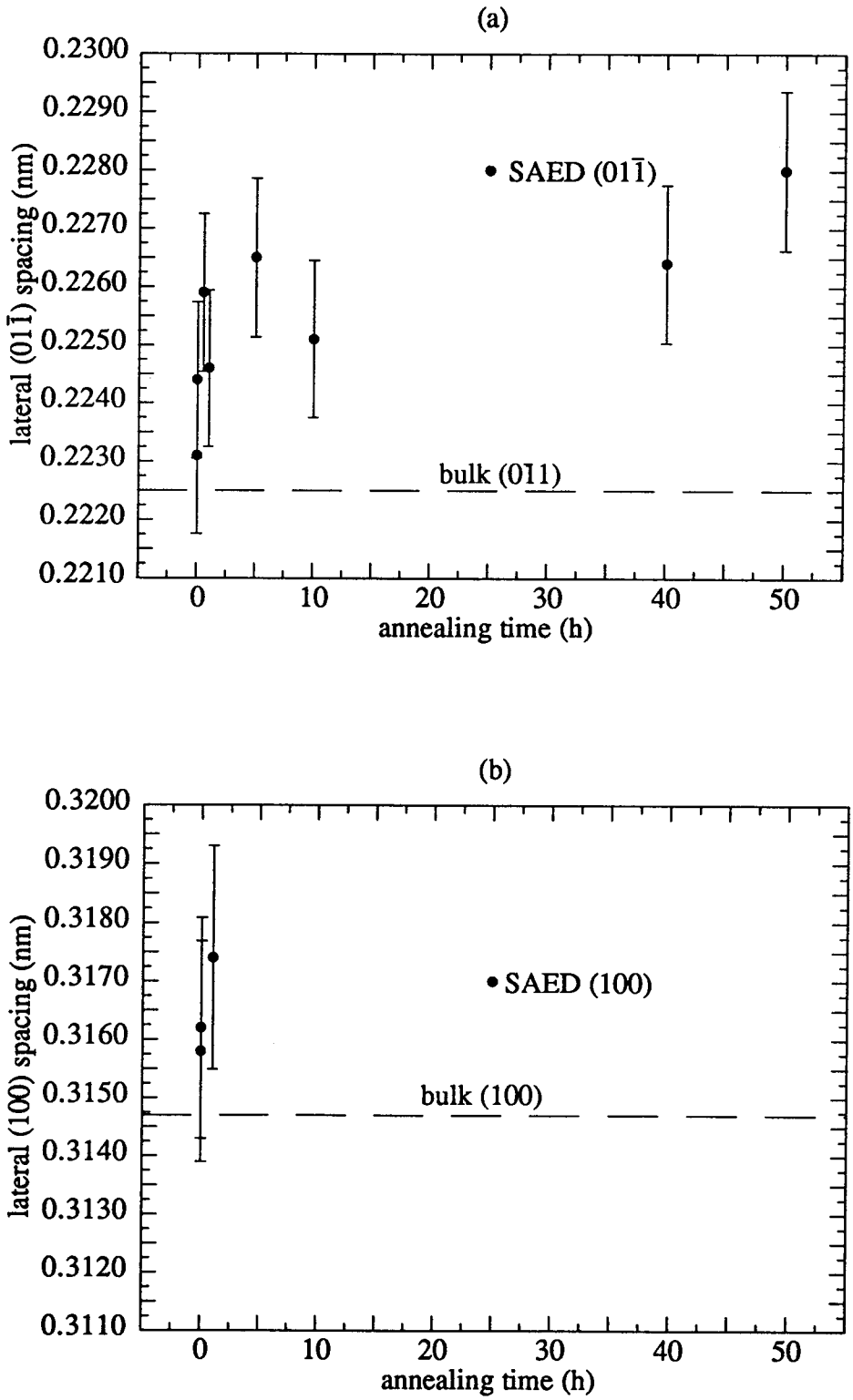

Figure 6 continued.

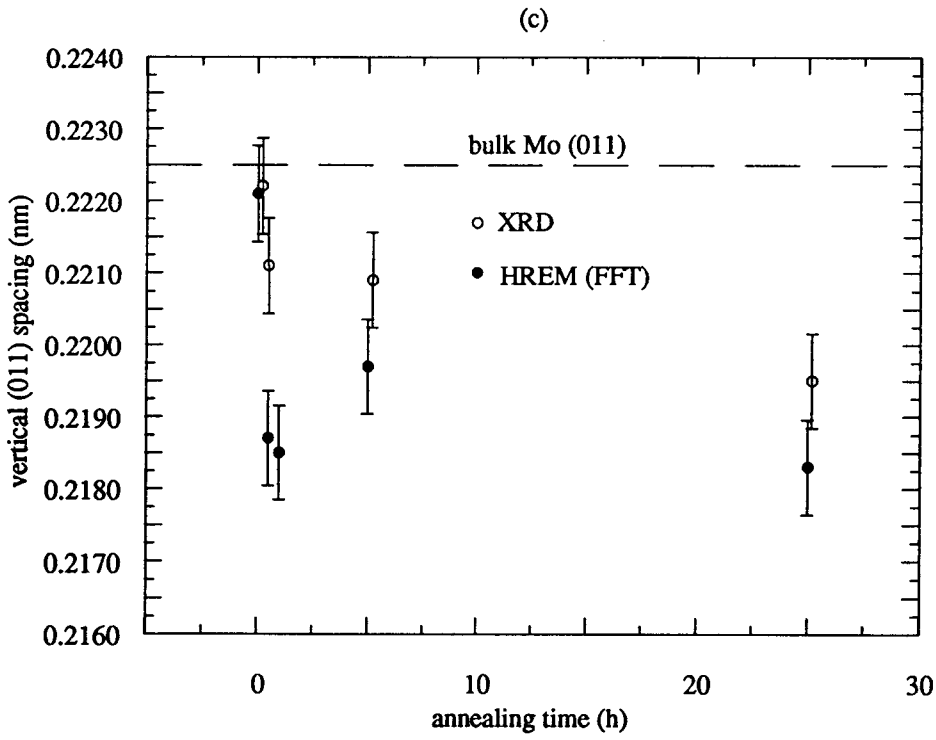

Figure 7 Lateral and vertical strains in Mo.

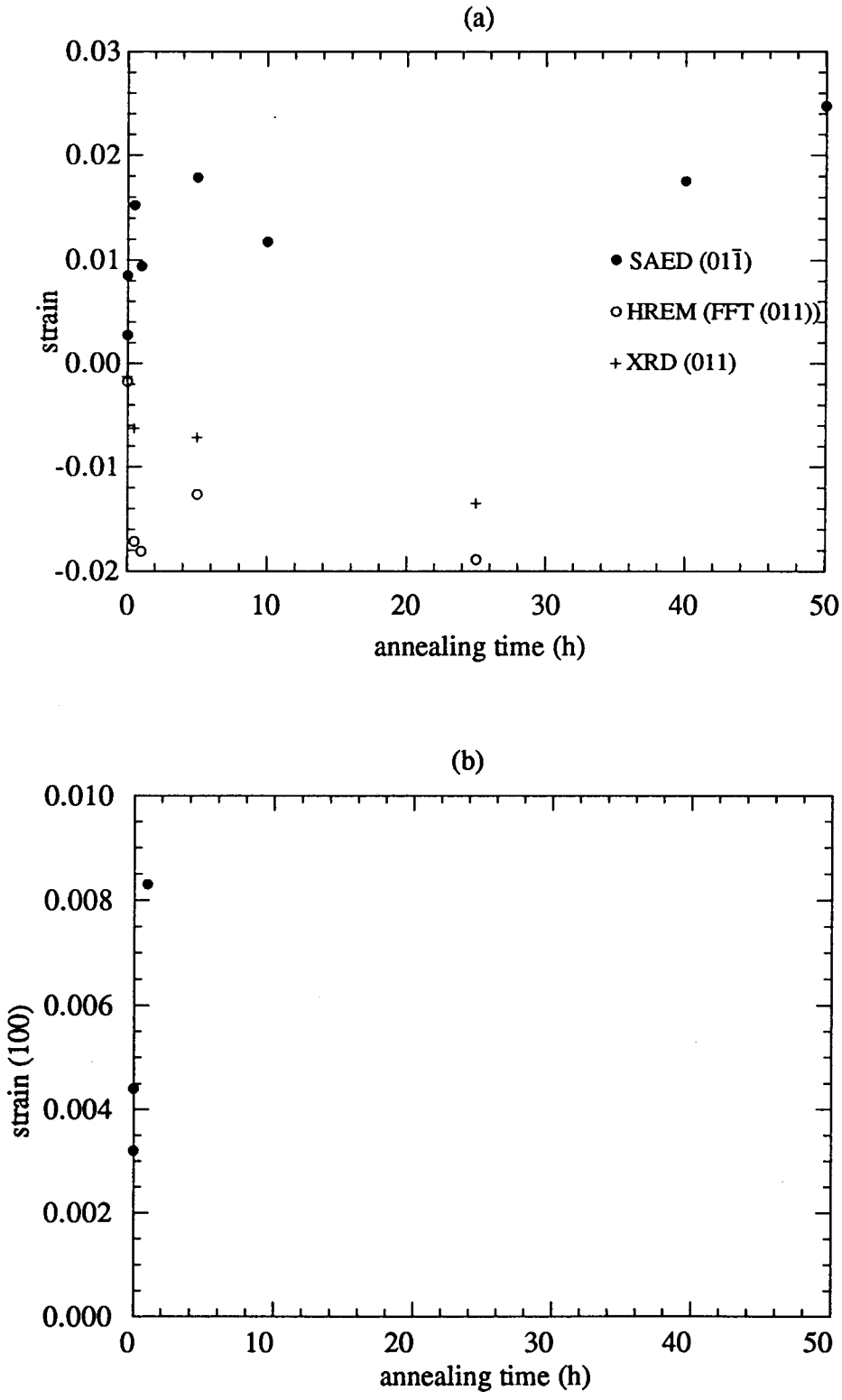

Table 1 Biaxial stress in ~0.1 μm layers as measured by laser deflectometry

layer description	layer thickness	unannealed	annealed	
			1/2 hour	10 hours
a-Si on SiO_2 of wafer	0.11 μm	-1360 MPa	-533 MPa	-379 MPa
Mo on a-Si on wafer	0.105μm	1140	826	834
a-Si on Mo on a-Si on wafer	0.11 μm	-1242	-30	-190

The as-deposited multilayers have thin amorphous interlayers at the Mo/a-Si interfaces which grow during annealing. The growth is relatively rapid in the primary stage and slow in the secondary stage. Large tensile strains in the lateral direction in the optical Mo layers are present in the as-deposited multilayer and increase with annealing. There is also a corresponding contraction in the vertical direction.

The secondary growth stage, in both types of interlayers, has been shown in earlier work [1,2] to be a diffusion controlled process with an activation energy of 2.4 eV. This corresponds to the activation energy for Si diffusion in h-$MoSi_2$ [14,15,17,18]. While the mechanisms for the more gradual growth is understood in terms of classic diffusion, the explanation for the initial, rapid growth surge is less clear. It involves growth of only 1-2 atomic layers on each side of the amorphous MoSi interlayer. This rapid growth also appears to be thermally activated [1], and may be associated with the increase in Mo residual stress.

Structural and/or composition changes in the interlayers cannot be easily assessed due to the amorphous nature and the very small dimensions. The relative speed of the short range growth may imply that the Mo and Si atoms adjacent to the Mo/a-Si interfaces are incorporated into the interlayer by rate-dependent atomic rearrangements and are different than those of the later, long-range diffusion of Si through the Mo-Si interlayer (e.g. different diffusion path, vacancy concentration, etc.). It is possible that part of the driving force for the surge is a rearrangement or reconstruction which results in a decrease in free energy with structural modification, kinetically facilitated by an increase in temperature The as-deposited interlayer may have an initial stoichiometry and amorphous structure that is relatively unstable. The above is certainly speculative, although interlayer formations (sometimes by amorphization) have been frequently observed (e.g. [19,20]).

A single crystal Mo film with a (011) plane parallel to the film plane will have anisotropic elastic properties in the plane of the film [5]. The stresses in two perpendicular directions in the plane of the film can be calculated by:

$$\sigma_{[100]} = C_{11}\varepsilon_{[100]} + C_{12}\varepsilon_{[01\bar{1}]} - \frac{2C_{12}^2\varepsilon_{[100]} + C_{12}(C_{11} + C_{12} - 2C_{44})\varepsilon_{[01\bar{1}]}}{(C_{11} + C_{12} + 2C_{44})} \quad (2)$$

$$\sigma_{[01\bar{1}]} = C_{12}\varepsilon_{[100]} + \frac{(C_{11} + C_{12} + 2C_{44})}{2}\varepsilon_{[01\bar{1}]} - \frac{(2C_{12}\varepsilon_{[100]} + (C_{11} + C_{12} - 2C_{44})\varepsilon_{[01\bar{1}]}}{2}\frac{(C_{11} + C_{12} - 2C_{44})}{(C_{11} + C_{12} + 2C_{44})} \quad (3)$$

where C_{11}, C_{12}, and C_{44} are the stiffness constants for Mo. These values are, respectively, 470, 168, and 107 GPa for bulk Mo [21].

The individual grains of the polycrystal have a random orientation about an axis perpendicular to the film and parallel to the [011] direction. The lateral Mo stress $\sigma_{[100]}$ is 2004 MPa while $\sigma_{[01\bar{1}]}$ was 1237 and 3096 MPa for the as-deposited multilayers. $\sigma_{[01\bar{1}]}$ = 6195 MPa at 0.5 hours. With one hour annealing, $\sigma_{[100]}$ increases to 4144 and $\sigma_{[01\bar{1}]}$ to 3173 MPa. At 5 hours $\sigma_{[01\bar{1}]}$ = 7288 MPa. With 10 hours and 50 hours, $\sigma_{[01\bar{1}]}$ is 4737 and 10960 MPa, respectively, assuming $\varepsilon_{[01\bar{1}]} = \varepsilon_{[100]}$ ($\varepsilon_{[100]}$ has a relatively small effect on $\sigma_{[01\bar{1}]}$ for comparable strain values). Since, as will be shown when the Poisson contractions are discussed, the higher as-deposited $\varepsilon_{[01\bar{1}]}$ strain is anomalous, the lower as-deposited $\sigma_{[01\bar{1}]}$ value in Mo may be more reliable. These are all based on the lateral strains indicated in Figures 7(a) and (b). The stress in the unannealed 0.1μm Mo layer was measured from laser deflectometry to be 1200 MPa. This is comparable to one (probably the more accurate) of the as-deposited stresses, indicating that adsorbed H_2O may not have an effect on the stress and also that activation of dislocation sources in thicker films is not important at ambient temperature. The decrease in tensile stress with annealing the 0.1μm Mo layers may have been due to thermal activation of dislocation sources [5]. It has been shown that thicker layers, above the critical thickness (e.g. >5 nm), allow for such sources [5]. Also, thermal activation may facilitate dislocation activity in layered films at elevated temperatures. The residual stresses in thin and thick amorphous Si layers are probably equal because of the absence of the dislocation relaxation mechanism, also providing the

absence of differences due to H_2O adsorption with each deposition pass and any change in structure (such as bulk defects with film thickness).

The data of Table 1 show that a-Si deposited on Mo and a-Si deposited on SiO_2 have similar residual stresses. The near equivalence suggests that, despite the thickness and growth-rate differences between the a-Mo-Si interlayers for Mo deposited on a-Si and a-Si deposited on Mo, the nature of the interfaces, in terms of structural features that lead to residual strains, appears identical.

Table 2 shows the measured residual stress in 40 bilayer multilayers as a function of annealing time. The as deposited multilayer residual stress of about -450 MPa is in good agreement with other work on Mo-Si multilayers of similar period and thickness on (111) oriented silicon substrates [6,7]. It can be noticed that the residual stress changes from about -450 MPa, for the as-deposited multilayer, to between +1500 and +2000 MPa with annealing (an anomalously high compressive stress of -15,312 MPa was observed after 20 min. annealing). The amorphous silicon in the as-deposited 0.1 μm layer is under a +1365 MPa residual stress. If the silicon layer is 3.06 nm thick, molybdenum is 2.33 nm thick and $MoSi_2$ is 1.5 nm thick, then the stress in the $MoSi_2$ is about -1800 MPa. After about 0.5 hours of annealing this changes to about -547 MPa and +763 MPa after 10 hours. This assumes multilayer and Mo layer stresses based on interpolation. (The anomalous 40 bilayer residual stress of about -15 GPa would seem to imply an a-$MoSi_2$ stress of about -40 GPa, which also appears anomalous.)

The ratio of the expected vertical strain to lateral strain based on a Poisson contraction can be calculated assuming that the Mo layers are monocrystalline, with a <110> direction perpendicular to the deposition plane. The ratios of vertical strains to lateral strain in this coordinate system are:

$$\frac{\varepsilon_{[011]}}{\varepsilon_{[100]}} = \frac{-4C_{12}C_{44}\sigma_{[100]} - (C_{11}^2 + C_{11}C_{12} - 2C_{12}^2 - 2C_{11}C_{44})\sigma_{[01\bar{1}]}}{4C_{44}((C_{11} + C_{12})\sigma_{[100]} - C_{12}\sigma_{[01\bar{1}]})} \qquad (4)$$

Table 2 Residual stresses in 40 bilayer optical multilayers versus annealing time at 316°C, measured by laser deflectometry

Annealing Time (hours)	Residual Stress (MPa)
0.0	-457
0.33	-15312
0.67	2066
1.0	1495
5.0	1612
25.0	1733

$$\frac{\varepsilon_{[011]}}{\varepsilon_{[01\bar{1}]}} = \frac{-4C_{12}C_{44}\sigma_{[100]} - (C_{11}^2 + C_{11}C_{12} - 2C_{12}^2 - 2C_{11}C_{44})\sigma_{[01\bar{1}]}}{-4C_{12}C_{44}\sigma_{[100]} + (C_{11}^2 + C_{11}C_{12} - 2C_{12}^2 + 2C_{11}C_{44})\sigma_{[01\bar{1}]}} \quad (5)$$

where C_{11}, C_{12}, and C_{44} are the stiffness constants at ambient temperature from [21]. Table 3 shows the expected values based on Eqs. (4) and (5). Average values of $\varepsilon_{[011]}/\varepsilon_{[100]}$ and $\varepsilon_{[011]}/\varepsilon_{[01\bar{1}]}$ (ignoring the anomalous -1.81 for one of the as-deposited lateral measurements) are between 0.85 and 0.9. The observed values are within reasonable agreement with predicted or theoretical values that are influenced somewhat by observed stresses (strains). Figures 8(a) and (b) illustrate the observed Poisson's ratio values. There is reasonable agreement between the observed values and the predicted values of about 0.85 to 0.90. These figures also illustrate the Poisson's ratio for the cases where the stresses are independent of the direction in the multilayer plane.

The lattice paramter of unstressed Mo in this multilayer system could concievably differ from that of bulk Mo [22]. A source of deviation could be Si dissolved into Mo. In this case both lateral and vertical "swelling" of the Mo lattice would be expected. However, vertical contraction in reasonable agreement with a calculated Poisson effect is seen. Also, the binary phase diagram for the Mo-Si system suggests that the solubility of Si in Mo at 316°C is essentially zero.

As discussed earlier, Kola et al. [4] suggested a plasticity mechanism facilitated by elevated temperature to rationalize the amorphous silicon film relaxation we observed. The question remained, however, as to the cause of the increase in tensile stress/strain in the thin Mo layers with annealing that these investigators failed to observe. One possible explanation is that the increase is due to the relaxation of compression stress in the amorphous Si layers [2] as shown in Table 1. However, the decrease in elastic strain energy in the Si layers is probably consumed by plastic deformation, which includes defect creation or annihilation and thermal losses in a-Si. As shown in Table 4, the elastic strain energy decrease in a-Si is comparable to the elastic strain energy increase in Mo. This suggests, therefore, that some other mechanism than a-Si relaxation by plasticity is

Figure 8 Vertical and lateral Mo strain ratios.

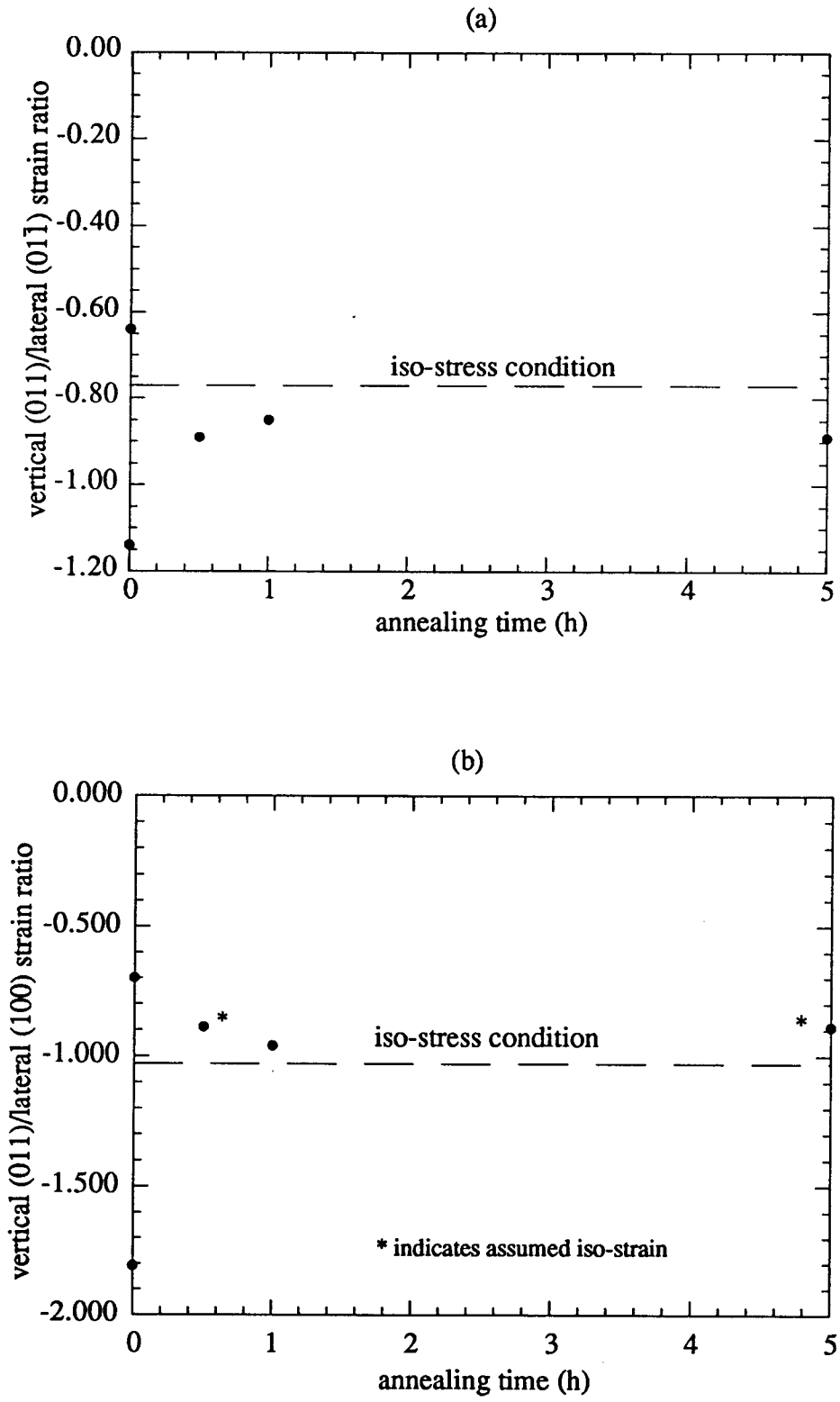

Table 3 Theoretical Poisson ratio as calculated using equations (4) and (5).

Annealing Time (hours)	$\varepsilon_{[011]}/\varepsilon_{[100]}$	$\varepsilon_{[011]}/\varepsilon_{[01\bar{1}]}$
0	-0.70	-1.14
0	-1.81***	-0.64***
1/2	-0.89**	-0.89
1	-0.96	-0.85
5	-0.89**	-0.89
average *	-0.86	-0.88

Notes: * -1.81 value omitted from average
** $\varepsilon_{[100]}$ assumed equal to $\varepsilon_{[01\bar{1}]}$
*** indicates probable erroneous measurements

Table 4 Change in elastic stress and strain energy in 40 bilayer optical multilayers.

	a-Si		Mo	
	unannealed	annealed 10 hours	unannealed	annealed 10 hours
average stress	-1494 MPa*	-417 MPa	2076(1620) MPa	4654 MPa
biaxial modulus	140 GPa		445 GPa	
thickness	3.06 nm	2.32 nm	2.33 nm	1.85 nm
strain energy	1.03 J/m^2	0.06 J/m^2	0.43 J/m^2	2.6 J/m^2
change in strain energy with annealing	--	-0.91 J/m^2	--	1.6 J/m^2

involved in establishing large tensile stresses in thin Mo layers in annealed optical multilayers.

Various studies have been performed [24,25] that observed an exothermic reaction with annealing a-Si at elevated temperatures, without crystallization. The heat released was between 3.7 and 17.5 kJ/mole, which yields 28-135 J/m^2 in the 40 layers of a-Si. These values are substantially larger that the net elastic strain energy increase (see Table 4). This suggests sufficient energy to induce tensile stress at the interface. That is, changes in the a-Si (e.g., defect structure, bond angle [24,25,27]) lead to changes at the interface which, in turn, lead to changes in the stress state. However, there is no direct evidence for a phase change. It, perhaps, should be mentioned that these exothermic reactions in a-Si may be associated with the plastic relaxation in the a-Si described by Kola et al. [4].

Another explanation relates to the amorphous Mo-Si interlayers. As mentioned earlier, it is possible that the initial growth surge is evidence for a reconstruction of local structural change in the amorphous interlayer over a few atomic distances, which induces strains in the Mo and a-Si layers. This phase change or reconstruction is enabled, kinetically, at higher temperatures It appears that the most pronounced stress increase is associated with the initial thickness surge. The enthalpy of formation of $MoSi_2$ is 43.9 kJ/mole [28], and this is a typical value for the enthalpy of formation of Mo-Si compounds [28]. Although the enthalpy associated with a reconstruction is unknown, it may be comparable to the enthalpy of formation of Mo-Si compounds. The magnitude of the energy release by the formation of the thin $MoSi_2$ after the relatively rapid thickness surge to 0.8 and 1.44 nm with annealing at 316°C corresponds to an energy increase of about $400J/m^2$ for 40 bilayers. Therefore, the driving force provided by the surge or reconstruction may be more than sufficient for the increase in the strain energy of the Mo layer (= 2 J/m^2). Crystallization of the amorphous Mo-Si phase does not appear to explain the stress changes. The crystallized volume after 50 hours of annealing is only 10 % (after 100 hours it is nearly 100 %). The residual stresses maximize at times less than 50 hours.

CONCLUSIONS

1. Annealing of optical Mo/a-Si multilayers results in growth and crystallization of amorphous Mo-Si interlayers.
2. The thin layers of the as deposited multilayer have substantial residual stresses: +1.2 to +2.0 GPa in the Mo and about -1.3 GPa in a-Si, based on HREM, SAED, XRD, and laser deflectometry methods. The $MoSi_2$ layers have an average residual stress of about -1.8 GPa.
3. The residual stresses in the Mo increase to abut 10 GPa, and in the a-Si decrease to about 0.5 GPa with 10 hour annealing at 316°C. The $MoSi_2$ appears to increase to about 0.8 GPa. The total residual stress in the optical multilayers increases substantially with 10 hour annealing at 316°C from -450 MPa to abut 2000 MPa.
4. These results have similarities with some other work that suggests stress relaxation in amorphous silicon by plasticity. Tensile stresses increase relatively rapidly in the thin Mo layers. The source of this increase is also unclear, but may be associated with and observed relatively rapid growth in the amorphous Mo-Si interlayers. The growth may be associated with a local (about 0.3 nm) rearrangement/reconstruction of the a-Mo-Si/Mo and a-Mo-Si/a-Si interfaces leading to changes in the stress state of the Mo layers, although other sources, such a structural changes in the amorphous silicon or crystallization of the amorphous Mo-Si must be considered.

BIBLIOGRAPHY

1. R.S. Rosen, D.G. Stearns, M.A. Villiardos, M.E. Kassner, S.P. Vernon, and Y. Cheng, *Appl. Optics 32*, 6975 (1993).

2. R.S. Rosen, D.G. Stearns, M.E. Kassner, J. Koike, Y. Cheng, and S.P Vernon, *J. Nano. Mater. 3*, 195 (1993).

3. D.G. Stearns, R.S. Rosen, and S.P. Vernon, *Proc. Multilayer Optics for Advanced X-Ray Applications, SPIE, 1547,* 2 (1991).

4. R.R. Kola, D.L. Windt, W.K. Waskiewcz, B.E. Weir, R. Hull, G.K. Cellar, and C.A. Volkert, *Appl. Phys. Lett. 60,* 3120 (1992).

5. W.D. Nix, *Metall. Trans. 20A,* 2217 (1989).

6. T.D. Nguyen, *Mater. Res. Soc. Symp. Proc. 343*, 579 (1994).

7. T.D. Nguyen, X. Lu, and J.H. Underwood, *Physics of X-Ray Multilayer Structures,* OSA Tech. Digest Series 6, 102 (1994).

8. J.A. Bain, L.J. Chyung, S. Brennan, and B.M. Clemens, *Phys. Rev. B 44*, 1184 (1991).

9. D.G. Stearns, R.S. Rosen, and S.P. Vernon, *J. Vac. Sci. Tech. A9*, 2662 (1991).

10. P.H. Townsend, D.M. Barnett, and T.A. Brunner, *J. Appl. Phys. 62*, 4438 (1987).

11. A.K. Petford-Long, M.B. Stearns, C.-H. Chang, S.R. Nutt, D.G. Stearns, N.M. Ceglio, and A.M. Hawryluk, *J. Appl..Phys. 61*, 1422 (1987).

12. K. Holloway, K.B. Do, and R. Sinclair, *J. Appl..Phys. 65*, 474 (1989).

13. J. Baglin, J. Dempsey, W. Hammer, F. d'Heurle, S. Peterson, and C. Serano, *J. Electron. Mater. 8*, 641 (1979).

14. J.Y. Cheng, H.C. Cheng, and L.J. Cheng, *J. Appl. Phys. 61*, 2218 (1987).

15. P.R. Gage, and R.W. Bartlett, *Trans. Metall. Soc. AIME 233*, 832 (1965).

16. A. Witvrouw and F. Spaepen, *Mat. Res. Symp. Proc. 205*, 21 (1992).

17. A. Guivarc'h, P. Auvray, L. Berthou, M. Le Cun, J.P. Boulet, P. Henoc, and G. Pelous, *J. Appl. Phys. 49*, 233 (1978).

18. E.P. Nechiporenko, E.P. Poltasev, N.S. Kapustin, V.V. Kapustin, and Yu T. Kondratov, *Izv. Akad. Nauk SSSR, Neorg. Mater. 10*, 1829 (1973).

19. T. Sands and A.S. Kaplan, *Appl. Phys. Lett. 50*, 1346 (1987).

20. F.Y. Sheau and Y.A. Chang, *Appl. Phys. Lett. 55*, 1510 (1989).

21. G. Simmons and H. Wang, *Single Crystal Elastic Constants and Calculated Aggregate Properties: A Handbook, 2nd ed.,* The MIT Press, Cambridge, MA, 1971.

22. B.M. Clemens and J.A. Bain, *MRS Bull. 17, No. 7,* 46 (1992).

23. M. Hansen and K. Anderko, *Constitution of Binary Alloys,* McGraw-Hill, New York, or General Electric Co., Business Growth Services, Schenectady (1958).

24. S. Roorda, W.C. Sinke, J.M. Poate, D.C. Jacobsen, P. Fuoss, S. Dierker, B.S. Dennis, and F. Spaepen, *Mater. Res. Soc. Symp. Proc. 157,* 683 (1990).

25. S. Roorda, S. Doorn, W.C. Sinke, P.M.L.O. Scholte, and E. van Loenen, *Phys. Rev. Lett. 62,* 1880 (1989).

26. W. Sinke, T. Warabisako, M. Miyao, T. Tokuyama, S. Roorda, and F. Saris, *J. Non-Cryst. Solids 39,* 308 (1988).

27. R. Tsu, J. Gonzares-Hernandez, and P.H. Pollak, *J. Non-Cryst. Solids 66,* 109 (1984), *Solid State Commun. 54,* 447 (1985).

28. T.G. Chart, *Metal. Sci. 8,* 344 (1974).